High-Pressure FTIR Study of the Stability of Horseradish Peroxidase. Effect of Heme Substitution, Ligand Binding, Ca^{++} Removal, and Reduction of the Disulfide Bonds†

L. Smeller,*,‡ F. Meersman,§ J. Fidy,‡ and K. Heremans§

Department of Biophysics & Radiation Biology, Semmelweis University, Puskin u. 9. PF 263, H-1444 Budapest, Hungary, and Department of Chemistry, Katholieke Universiteit Leuven, Celestijnenlaan 200D, B-3001 Leuven, Belgium

Received May 24, 2002; Revised Manuscript Received October 31, 2002

ABSTRACT: The pressure stability of horseradish peroxidase isoenzyme C and the identification of possible stabilizing factors are presented. The effect of heme substitution, removal of Ca^{2+}, binding of a small substrate molecule (benzohydroxamic acid), and reduction of the disulfide bonds on the pressure stability were investigated by FTIR spectroscopy. HRP was found to be extremely stable under high pressure with an unfolding midpoint of 12.0 ± 0.1 kbar. While substitution of the heme for metal-free mesoporphyrin did not change the unfolding pressure, Ca^{2+} removal and substrate binding reduced the midpoint of the unfolding by 2.0 and 1.2 kbar, respectively. The apoprotein showed a transition as high as 10.4 kbar. However, the amount of folded structure present at the atmospheric pressure was considerably lower than that in all the other forms of HRP. Reduction of the disulfide bonds led to the least pressure stable form, with an unfolding midpoint at 9.5 kbar. This, however, is still well above the average pressure stability of proteins. The high-pressure stability and the analysis of the pressure-induced spectral changes indicate that the protein has a rigid core, which is responsible for the high stability, while there are regions with less stability and more conformational mobility.

We investigated the possible structural source of the unusually high-pressure stability of horseradish peroxidase. High pressure is often used as an external perturbation in protein studies (*1*, *2*). Depending on the pressure range, the extent of the changes in the structure of globular proteins may be different. Moderate pressures (typically from ambient pressure to 5−10 kbar, depending on the actual protein) distort the secondary and tertiary structure of the polypeptide, without abolishing its specific biological activity (elastic effect) (*3*, *4*). Higher pressures can lead to denaturation of the protein, by inducing the loss of the secondary structure (conformational effect) (*5*−*8*). Pressure studies contribute both to the basic knowledge about the conformation and stability of proteins and open fields of practical applications (*9*−*13*).

Horseradish peroxidase (HRP)[1] is a heme protein, which catalyzes the H_2O_2-dependent oxidation of aromatic electron donor molecules. Its crystal structure was recently determined by Gajhede et al. (*14*) and further refined by computer modeling (*15*). The structure of HRP in its complexed form with benzohydroxamic acid (BHA) (*16*) and with ferrulic acid (*17*) as substrates is also known. These results show that the major structural elements in the protein are α-helices (*15*). Additionally there are two Ca^{2+} ions bound to the protein (*18*, *19*). Studies by Morishima and co-workers show that at least one Ca^{2+} is needed for the full activity of the enzyme (*18*, *20*).

HRP is known as a fairly stable protein against temperature and pressure denaturation (*21*−*23*). Holzbaur et al. (*21*) investigated the effect of heating on HRP using infrared spectroscopy. They found that Fe(III)HRP unfolds between 85 and 90 °C. Recent DSC and CD studies showed a lower unfolding temperature (56 °C−64 °C depending on the heating rate) at pH 3 (*24*). A special feature of the HRP is that unlike most of the proteins, heat-unfolded HRP molecules do not form intermolecular hydrogen bonds (*21*). Kaposi et al. (*25*) studied the effect of Ca^{2+} removal, and binding of benzohydroxamic (BHA) acid to HRP in the temperature range of 10−300 K.

Several studies have been performed on the enzymatic function of peroxidases. The activity of peroxidases from different fruits were determined after pressure treatment (*26*−*28*).

Methods based on high-resolution fluorescence spectroscopy require the heme in HRP to be substituted, by a metal porphyrin with closed electron shell (Mg^{2+}, Zn^{2+}), or by a metal-free porphyrin (*13*, 29). These substituted forms of HRP were used to determine the internal isothermal compressibility of HRP and other proteins in the low-pressure (*30*, *31*) and high-pressure range (*32*) by high-resolution

† This work has been supported by the Hungarian National Research Foundation OTKA T032117 Project and by the Fund for Scientific Research-Flanders (Belgium). L.S. thanks the Hungarian Academy of Science for travel grants.

* Corresponding author.
‡ Semmelweis University.
§ Katholieke Universiteit Leuven.

[1] Abbreviations: HRP, horseradish peroxidase; BHA, benzohydroxamic acid; NHA, naphthohydroxamic acid; MgMP, magnesium mesoporphyrin; FTIR, Fourier transform infrared spectroscopy; EDTA, ethylenediaminetetraacetic acid; DTE, dithioerythritol.

10.1021/bi026192n CCC: $25.00
Published on Web 12/17/2002

optical spectroscopy. One of the questions we address in the present study is whether major conformational changes or other alterations (e.g., in the pressure stability) take place in the protein as consequence of the substitution of the heme by metal-free mesoporphyrin (MP).

There are number of small aromatic molecules which can bind in the heme pocket. One of them is BHA. This small aromatic molecule is known to bind near the heme. X-ray crystallographic data (*16*) indicate only a very small change of the secondary structure as consequence of the binding. Recent studies by computer simulation techniques showed only differences in side chain dynamics between the complexed form with BHA and with a similar other substrate, naphthohydroxamic acid (NHA) (*15*).

An early pressure study on horseradish peroxidase was performed by Ogunmola et al. (*22*). Their highest technically reachable pressure was 8 kbar. At this pressure the completely unfolded state was not reached. Our present experiment covers the whole pressure range, where the water is liquid (up to ~13 kbar at room temperature).

In this study we follow the conformational changes in the secondary structure of horseradish peroxidase by FTIR spectroscopy during pressurization. Several different structural forms of HRP were compared: the native form complexed with BHA, the protein after heme substitution, the Ca^{2+} -depleted form and the structure after reducing the disulfide bonds. The aim of the present study is to investigate how these factors contribute the pressure stability.

EXPERIMENTAL SECTION

Horseradish peroxidase (HRP) was purchased from Sigma (RZ = 3.0). To purify the basic form (isoenzyme C) of this protein, column chromatography was used (*33*). The protein was applied to a CM Sepharose (Pharmacia) in a column equilibrated with 5 mM Tris buffer at pH 7.4 and eluted with 0.01 M NaCl. The RZ values of the fractions were checked by a Cary 4E (Varian) absorption spectrophotometer and the fraction RZ = 3.4 was used.

The native heme group was removed from the enzyme by acid methyl ethyl ketone (*34*) to obtain apoHRP. For the heme-substituted protein (MP−HRP), the apoprotein was reconstituted with aliquots of metal-free mesoporphyrin (MP) dissolved in ethanol. The solution was lyophilized. The MP used in the substitution was produced by Porphyrin Products (Logan, UT). EDTA (disodium salt), the substrate BHA, and dithioerythritol (DTE) used in reduction of the enzyme were purchased from Sigma.

The samples for FTIR spectroscopy were prepared by dissolving the lyophilized protein in 10mM deuterated acetate buffer (pD 5.0) at 75 mg/mL. Heavy water (D_2O) was used for all measurements in order to avoid the interference of the strong water band at 1640 cm^{-1} with the analyzed amide I band. The pH meter was calibrated by reference to standard buffers in H_2O and the reading was corrected for the deuterium isotope effect according to pD = pH meter reading +0.4. The sample was stored overnight to ensure sufficient H/D exchange. The pH of the solution was controlled before it was used for the measurement. The protein solution was centrifuged a few minutes before use.

To remove the Ca^{2+} from the protein EDTA was added to the protein solution in a molar ratio of EDTA:protein = 10:1. This sample is called Ca^{2+}-free; however, the completeness of the removal is discussed in the Discussion section.

For the reduction of disulfide bonds, DTE was added to the protein solution a few minutes prior to filling the pressure cell. The molar ratio of DTE to protein was 100:1 in the final sample.

FTIR Spectroscopy. The infrared spectra were obtained with a Bruker IFS66 FTIR spectrometer equipped with a liquid nitrogen cooled broad band MCT solid-state detector. 256 interferograms were co-added after registration at a resolution of 2 cm^{-1}.

High pressure was generated in a diamond anvil cell (Diacell Products, Leicester, U.K.), where the pressure was built up by means of a screw mechanism. Barium sulfate was used as an internal pressure standard in all cases (*35*). All experiments were performed at 25 °C.

The broad band of water around 3350 cm^{-1} was used to control that the solvent is still in the fluid phase even at the highest pressure used in the experiments. No crystallization was observed in the experiments reported here.

Data Processing. The overlapping components of the amide I/I′ band were resolved by the Fourier self-deconvolution developed by Kauppinen et al. (*36*). This is a mathematical transformation, which decreases the width of the component lines of the amide band. The optimal parameters were determined from the observation of the power spectrum as described by Smeller et al. (*37*). A resolution enhancement factor (*36*) of 1.5 was reached using the Lorentzian band shape of 20 cm^{-1} bandwidth. The deconvoluted spectra were then fitted with Gaussian functions. A good fit of the amide I region was achieved by six components. The fitting of component peaks was performed by a program developed in our laboratory, using the Levenberg−Marquard algorithm (*37*). The area of the fitted Gaussian lines was used in the quantitative secondary structure analysis.

RESULTS

Infrared Spectra of the Native HRP. Figure 1 shows the amide I/I′, II, and II′ regions of the infrared spectra of native HRP during pressurizing and depressurizing between atmospheric pressure and to 14 kbar. The spectrum measured at ambient pressure contains the conformation sensitive amide I/I′ band at 1651 cm^{-1} and two bands in the amide II/II′ region at 1550 and 1456 cm^{-1}. The amide I/I′ band which is characteristic for the secondary structure originates predominantly from a C═O stretching vibration. The amide II mode (1550 cm^{-1}) includes NH in plane bending (49%) (*38*) and is therefore very sensitive to hydrogen−deuterium (H/D) exchange. The corresponding deuterated (amide II′) band can be seen at 1456 cm^{-1}, ~100 cm^{-1} lower than the amide II frequency. The small bandat 1517 cm^{-1} (visible only in the deconvoluted spectrum) comes from the tyrosine ring vibrations (*39*).

Looking at the spectra of HRP (Figure 1), one can see that the characteristic infrared peaks change significantly under pressure. At 14 kbar a much broader amide I/I′ band can be observed. This broadening is accompanied by a shift of the band, caused by the decrease of the component band at higher wavenumber. Simultaneously, the component

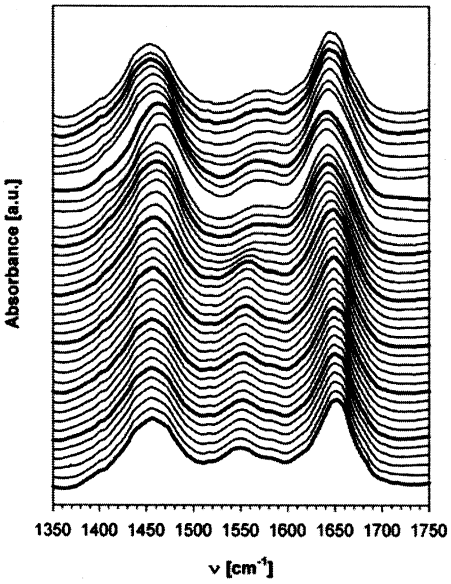

FIGURE 1: Stacked plot of the infrared spectra of native HRP at 25 °C. The pressures in kbar are from bottom to the top: **0.5**, 0.8, 1.3, 1.9, 2, **2.2**, 2.7, 3, 3.2, 3.3, **3.8**, 4.3, 5.2, 5.9, 6.5, **7.1**, 7.8, 8.5, 9.2, 10.3, **11**, 11.9, 12.2, 13, 13.4, **13.7**, 13.9, 14.3, 12.7, 11.2, **10.3**, 8.9, 7.3, 5, 3.1, **1.9**, 0.7.

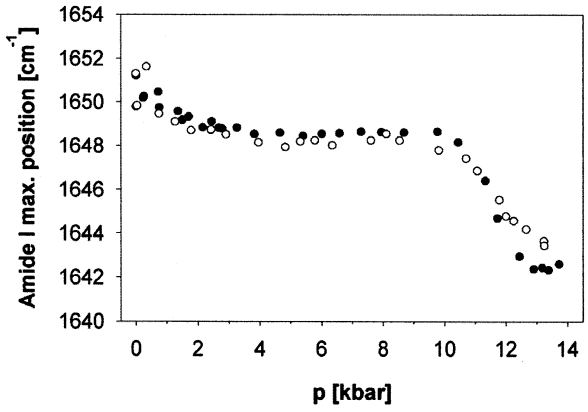

FIGURE 2: The maximum position of the amide I/I′ band vs pressure for the native (●) and the metal-free porphyrin containing (○) HRP.

characteristic for the disordered structure increases, which gives a broad peak at ca. 1640 cm^{-1}.

The maximum position of the overall amide I/I′ band is plotted as the function of the pressure in Figure 2. After an initial gradual shift, it remains constant, up to 10 kbar, where the unfolding starts. Above this pressure, the amide band position shifts significantly, following a sigmoid curve, with a midpoint at 12.0 ± 0.1 kbar. The bandwidth also increases sigmoidally at the same pressure (not shown). The shift and the broadening of the band are not reversible during depressurizing of the sample to atmospheric pressure.

A more detailed analysis of the amide I/I′ band can be obtained from Fourier self-deconvolution and band fitting. (*40*, *41*). The deconvoluted amide I/I′ band of HRP is dominated by two intense components: at 1646 and 1659 cm^{-1} (see solid lines in Figure 3). Analyzing the deconvoluted spectra, in the pressure range below 10 kbar, one can see a gradual change in the relative areas (*A*) of the 1659 and 1647 cm^{-1} bands. The ratio A_{1659}/A_{1647} is decreasing during the pressurization, and it shows a sigmoidal transition at 5 kbar (data not shown).

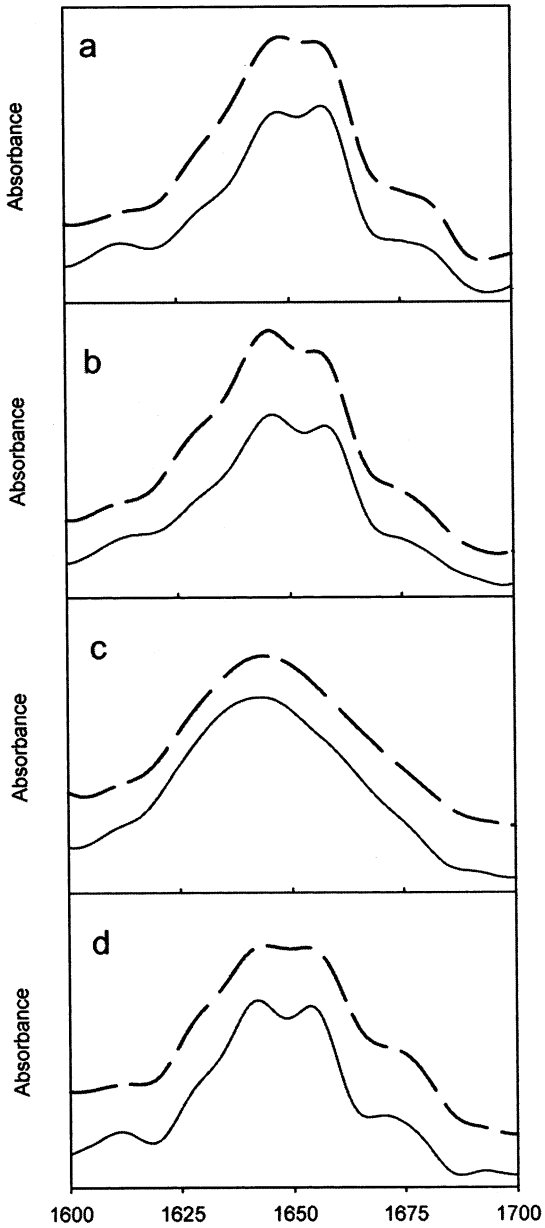

FIGURE 3: Deconvoluted amide I/I′ band of native (solid line) and metal-free porphyrin HRP (dotted line). Pressure values are as follows: (a) ambient pressure; (b) 5 kbar; (c) 13 kbar; (d) released to ambient conditions.

Above the unfolding pressure (12 kbar), the components of the amide I/I′ band cannot be resolved, indicating the loss of native secondary structure. After depressurizing the two bands become visible again, but they are shifted to lower wavenumbers (1641 and 1655 cm^{-1}).

As mentioned before, the amide II band (around 1550 cm^{-1}) originates from the vibration of the nondeuterated residues. One can observe an intensity decrease of this band simultaneously with the shift of the amide I/I′ band.

Metal-Free Porphyrin HRP. At ambient pressure the maximum position of the nondeconvoluted amide I/I′ band is at 1651 cm^{-1} both for the native form and for the enzyme which is substituted with metal-free porphyrin (MP−HRP).

Figure 2 also compares the position of the amide I/I′ band maximum for the native and MP−HRP. At ambient pressure the maximum of the amide I/I′ band is at 1651 cm^{-1} for both forms of the protein. After the start of the pressurization

Table 1: Pressure Stability of the Various Forms of HRP and the Ratio of Areas of the Amide I/I′ Components at 1659 and 1647 cm^{-1}

HRP	$p_{1/2}$	A_{1659}/A_{1647}
native	12.0 ± 0.1	0.85
metal-free porphyrin	11.7 ± 0.7	0.5
apo	10.4 ± 0.4	NA[a]
native + EDTA	10.0 ± 0.1	0.80
native + BHA	10.8 ± 0.1	0.98
reduced	9.5 ± 0.3	0.66

[a] NA: not available.

(below 3 kbar), one can observe a small decrease of the amide I/I′ band maximum position, and the broadening of the amide I/I′ band in the case of both proteins (data not shown). At the denaturation pressure, the maximum position drops to the value characteristic for the unfolded structure (around 1642 cm^{-1}). Simultaneously, the spectrum above the unfolding pressure (13 kbar) shows a considerable broadening. A fit of a sigmoidal function to the amide I/I′ band maximum position versus pressure gives a transition midpoint of 11.7 ± 0.7 kbar. This does not differ significantly from the value found for the native enzyme.

Figure 3 also compares the deconvoluted spectra of the native form and that of the enzyme substituted with metal-free porphyrin (MP−HRP). The deconvoluted spectra show that the two main components appear at 1659 and 1646 cm^{-1} at ambient pressure in both proteins. The relative intensities of the bands at 1659 and 1646 cm^{-1} are slightly different in the two variants of HRP. The native protein has a more intense band at 1659 cm^{-1}, while in the case of MP−HRP the other component gains intensity. The area ratios of the bands (A_{1659}/A_{1646}) are summarized in the Table 1 for all the studied cases.

The difference in the ratios A_{1659}/A_{1646} of the native and MP−HRP disappears during pressurization to 5 kbar, which is well below the denaturation pressure. This can be seen in Figure 3b, which compares the deconvoluted spectra of the native and MP−HRP at 5 kbar. The ratio of these component bands does not differ between 5 and 9 kbar. At 10 kbar the unfolding starts for both proteins and the components cannot be resolved any more.

Effect of High Pressure on apoHRP. In the case of apoHRP, the two components (1647 and 1659 cm^{-1}) cannot be resolved at ambient conditions, even in the deconvoluted spectrum. The maximum position of the deconvoluted spectrum is at 1644 cm^{-1}, which indicates the dominance of the unfolded component. We have to mention, however, that the sample of apoHRP that we used was slightly aggregated at low pressures, which also could contribute to the low secondary structure content. This is probably due to the partial destabilization of the 3D structure, which resulted in the partial unfolding of one domain of the protein. Such unfolded parts can build intermolecular interactions, which can lead to the aggregation. The aggregation is indicated by the appearance of the specific bands on both sides of the amide I/I′ band (1616 and 1685 cm^{-1}) (*42*). This aggregation explains the relatively low amide I/I′ maximum position and the slight increase of it below 2 kbar. The sidebands disappear around 2 kbar because this pressure is able to dissociate the protein aggregates (*5*).

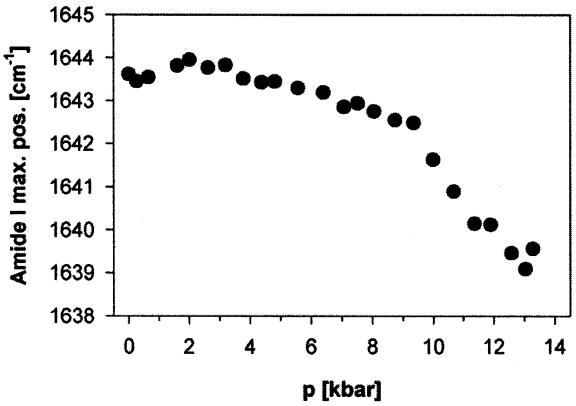

FIGURE 4: The maximum position of the amide I/I′ band vs pressure for the apo HRP.

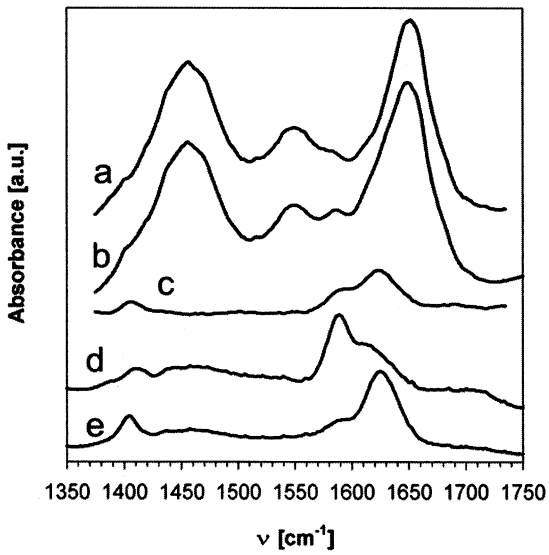

FIGURE 5: Infrared spectrum of (a) Ca^{2+}-bound HRP, (b) HRP+EDTA, (c) difference spectrum of b−a, (d) EDTA (18mM), and (e) EDTA + $CaCl_2$ (1:2 molar ratio).

The maximum position of the amide I/I′ band of apoHRP vs pressure is shown in Figure 4. The midpoint of the sigmoid shaped transition was found to be 10.4 ± 0.3 kbar, which is lower than the value found for the two types of holoproteins. Below this pressure, a slight, continuous pressure shift of the maximum of the amide I/I′ band was also observed.

Effect of Ca^{++} Removal. Figure 5a shows the amide I/I′, II, and II′ regions of the infrared spectrum of native HRP. The spectrum measured after the Ca^{2+} removal by EDTA, and the difference spectra are also plotted. For comparison the spectra of EDTA (18mM) and EDTA (18 mM) + Ca^{2+} (36 mM) are also shown. The characteristic bands of the Ca^{2+}-free (1624 and 1404 cm^{-1}) and Ca^{2+}-bound EDTA (1588 and 1406 cm^{-1}) can be clearly identified. These can be attributed to the asymmetric and symmetric stretching modes of the carboxylate, respectively (*25*). In the difference spectrum of HRP and HRP + EDTA, one can identify three peaks in the region of 1400−1625 cm^{-1} at the positions of 1406, 1588, and 1624 cm^{-1}. The 1624 cm^{-1} peak is due to the Ca^{2+}-free form of the EDTA, and the less intense 1588 cm^{-1} peak shows the presence of the Ca^{2+}-bound EDTA. The position of the amide I/I′ band is not changed upon removal of the Ca^{2+}, which is in accordance with earlier

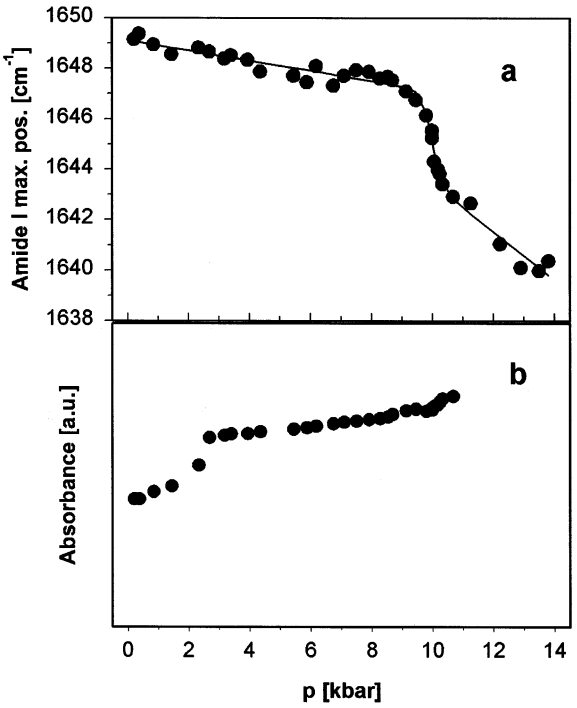

FIGURE 6: (a) The amide I/I′ peak position and (b) intensity of the 1588 cm^{-1} band vs pressure for the Ca^{2+}-free HRP.

reports (*25*). The increased intensity ratio of 1646 and 1660 bands shows, however, a partial loss of the secondary structure.

Figure 6a shows the maximum position of the amide I/I′ band during the pressure treatment after Ca^{2+} removal. A sigmoidal behavior can be seen with a midpoint at 10.0 ± 0.1 kbar. This is significantly lower than that of the native form. A difference is also observed at pressures below the unfolding pressure. In this region a gradual shift of the maximum position can be observed. An abrupt decrease of the amide II band (1546 cm^{-1}) intensity can be observed at 10.0 kbar, the same pressure where the amide I/I′ band shifts and broadens.

The intensity of the 1588 cm^{-1} band is plotted in Figure 6b. One can observe a marked intensity increase at 2 kbar.

Effect of BHA Binding. The binding of BHA is not accompanied by a marked spectral change, which can be attributed to the ligand binding (data not shown). The maximum position of the band is also not affected by the ligand binding. The secondary structure analysis shows a small increase of the helical structure (1659 cm^{-1} band) compared to the disordered one (1648 cm^{-1} band).

Figure 7 shows the maximum position of the amide I/I′ band versus pressure for BHA bound protein. The maximum position of the amide I/I′ band is lowered as consequence of the substrate binding above 5 kbar. This shift is further enhanced as the pressure is increased. The unfolding pressure of substrate bound HRP is also smaller than that of the substrate free enzyme. In the presence of substrate, the transition is at 10.8 ± 0.2 kbar, which is between the stability of the native and the Ca^{2+}-free protein. Again the shift of the amide I/I′ band at the unfolding pressure is accompanied with the decrease in the amide II band amplitude, indicating the completion of the H/D exchange.

Effect of Reducing the Disulfide Bonds. When DTE was added to the system in order to reduce the disulfide bonds,

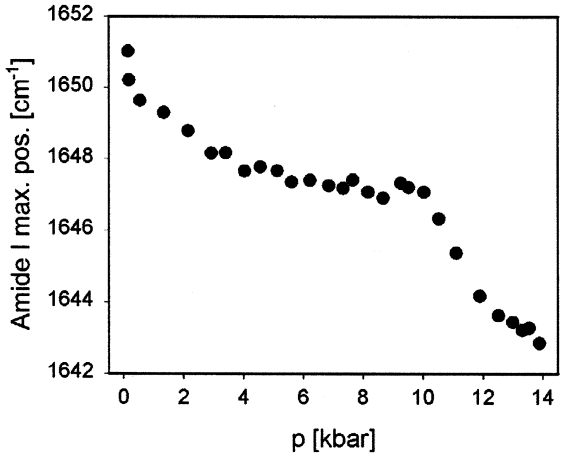

FIGURE 7: The maximum position of the amide I/I′ band vs pressure for HRP binding substrate benzohydroxamic acid.

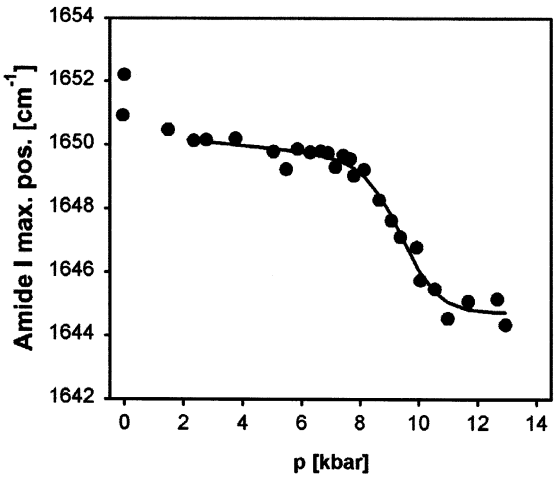

FIGURE 8: The amide I/I′ peak position values vs pressure for the HRP with reduced disulfide bonds. The fitted sigmoid curve is also shown.

again no major spectral changes were observed at ambient pressure. The maximum position of the amide I/I′ band was found in the same position as for the native enzyme. Curve fitting to the deconvoluted spectrum, however, resulted in a considerably lower A_{1659}/A_{1647} value (Table 1).

Figure 8 shows the amide I/I′ maximum position during the pressurization of the reduced enzyme. The midpoint of the fitted sigmoid curve is at 9.5 ± 0.3 kbar, which is the lowest among the studied forms. Again a shift of the spectral maximum to the lower wavenumbers is observed at low pressures. Upon returning to atmospheric pressure, the spectrum shows specific sidebands of the amide I/I′ band (1616 and 1685 cm^{-1}). These are characteristic for the intermolecular antiparallel β-sheet aggregation (*42*). Appearance of these high-intensity bands after the release of the pressure was not seen in any of the other forms of the HRP except for apoHRP, where they were already present with low intensity at the beginning of the experiment.

DISCUSSION

Native HRP. The amide I/I′ band of the proteins is the most conformation sensitive feature of their infrared spectrum. It is well-known that it contains several component bands whose contribution to the total area of the band is

proportional to the amount of the corresponding secondary structure assigned to the given component bands (*40*−*45*). Therefore, we first discuss the assignment of the resolution enhanced amide I/I′ band of HRP which is dominated by two component bands at 1646 and 1659 cm^{-1}. The latter can be assigned to the helical structure (*40*, *43*−*45*). According to the widely accepted assignments of the amide I/I′ components (*40*, *43*−*45*), the band around 1646 cm^{-1} is assigned to disordered, irregular structure. An unfolded protein is also characterized by single broad peak around this position (*45*). Although our component at 1646 cm^{-1} is not as broad as the amide I/I′ band of an unfolded protein, it is considerably broader than the component at 1659 cm^{-1} assigned to the α-helical parts of the protein. This also supports the assignment of the 1646 cm^{-1} band to an irregular structure.

Since the X-ray structure of HRP is known, we can compare the secondary structure content obtained as the result of the above assignment with the data provided by crystallography. According to X-ray crystallography (*14*), 51% of the amino acids are arranged in helices (44% in α-helix, 7% in 3_{10} helix), and there is a very small (<2%) *β*-sheet content, which means that 47% of the amino acids cannot be assigned to well-defined structures. The relative area of the 1659 cm^{-1} band, however, is significantly smaller (29%). This can be explained by taking into account that HRP contains a large number of helices. The effect on the amide I/I′ band can be explained as follows. In a folded α-helix, the length of the C═O bond, and therefore the force constant of the vibration, is influenced by the hydrogen bonding. The hydrogen bonded C═O is elongated, and the vibrational frequency decreases compared to the nonbound case. If the protein is in an aqueous solution, all of the oxygen atoms are hydrogen bonded, either with another part of the protein or with the surrounding water molecules. When bound to water, the C═O bonds are less uniform; that is why the amide I/I′ band of the unfolded proteins is quite broad. In an α-helix all the C═O bonds are directed more or less parallel to the main axis of the helix. In this helix the oxygen atom of the *i*-th amino acid is hydrogen bonded to the hydrogen of the *i*+4-th one. This means, that the last four amino acids of each helix do not have such a binding possibility within the helix; therefore, four amino acids at the end of the helix do not show the amide I/I′ vibration at the position characteristic for the helix. Taking into account that there are 12 α−helices in the HRP, the number of C═O groups in α-helix like hydrogen bonding is 88, i.e., 29% of the total number of amino acids. This corresponds to the experimental value we found. We have to note that Dousseau and Pezolet (*46*) found an improved correlation between the X-ray structure and the secondary structure content determined from the IR measurements if they assigned the first and last two amino acids to a structure which they called "disordered helix". Mathematically their result is the same as ours, but our explanation is based on the physical feature of the IR measurement, i.e., that the analyzed IR band is sensitive for the C═O···H part of the protein backbone.

Four of the five 3_{10} helices present in HRP are very short, and only one of them contains 6 interhelix hydrogen bonds. Studies on synthetic peptides forming 3_{10} helices reported amide I/I′ absorption at 1665 cm^{-1} (*47*). This weak component with an expected intensity of 2% in a strongly overlapping position cannot be resolved, even with the used resolution enhancement technique.

Turns and bends are responsible for the high-frequency component of the amide I/I′ band (around 1680 cm^{-1}). The rest of the amino acids give the absorption shown at 1646 cm^{-1}. Therefore, we assign this component to water-exposed, rather randomly oriented amino acids, which connect the helices. This assignment is in agreement with both the accepted (*40*, *43*−*45*) and calculated (*48*) infrared band positions, and the result is also in accordance with the X-ray structure of HRP.

The exchange of amide hydrogens to deuterium atoms can be followed using the amide II and the corresponding deuterated (amide II′) band. These are well separated in the spectrum; they appear at 1550 and 1450 cm^{-1}, respectively. The exchange is not completed at atmospheric pressure despite the overnight incubation of the sample in D_2O. This is clearly seen from the fact that the intensity of the amide II band (around 1550 cm^{-1}) decreases upon unfolding (Figure 1.). This suggests the presence of a rigid domain in the protein, which is not performing dynamic movements large enough for the exchange at ambient conditions. Recent molecular dynamics calculations also supported the presence of a rigid core in the molecule (Q. Huang, M. Laberge, J. Fidy, R. Schweittzer-Steiner, unpublished results). Similar nonhomogeneity of HRP was described recently, showing that there are domains with different compressibility in HRP (*32*). Since compressibility and fluctuations are closely related to each other by the fluctuation−dissipation theorem, domains with lower compressibility have reduced fluctuations and consequently lower rate of H/D exchange.

The downshift of the amide I/I′ components after pressure release is also the consequence of the exchange. The incomplete exchange before pressurizing can be one of the reasons for the slightly increased frequencies of the amide I/I′ components compared to the literature values.

HRP with its unfolding pressure of 12 kbar is a rather stable protein compared to other proteins studied so far under pressure (*49*−*52*). There are only few proteins with comparable or even higher pressure stability; one of them is the bovine pancreatic trypsin inhibitor (BPTI) (*53*), which is stabilized by two disulfide bonds. Disulfide bonds, however, are not always needed for the high stability, as it is shown on the example of P2 protein from the archaeon *Sulfolobus solfataricus* (*54*). It may be, however, of significance that both BPTI and P2 are small proteins. This is the first example of a protein with 306 residues that shows such extreme pressure stability.

Below 10 kbar there are slight changes in the secondary structure. The changes of the relative areas of the 1647 and 1659 cm^{-1} components can be interpreted as a small transition involving partial unfolding of the soft part of the protein at 5 kbar. Because there is no change in the amide II band intensity, the structural changes occur in the soft domain, where the H/D exchange has already been completed at atmospheric pressure. The component at 1659 cm^{-1} remains clearly present up to pressures higher than 10 kbar. This indicates that only a small part of the helices unfolds at 5 kbar and a considerable amount of the secondary structure persists in a very stable domain.

The HRP molecule contains five tyrosine residues. After a slight decrease below 2 kbar, the tyrosine band position

shows a linear blue shift with a rate of 0.35 cm^{-1}/kbar (data not shown). The linear shift to the higher frequencies can be explained by a pure physical effect of the pressure, which results in the compression of the bond lengths (*55*). The linear behavior of the pressure-induced shift of the tyrosine vibrational frequency means that the environment of the tyrosine does not change significantly below the unfolding. At the unfolding, the frequency decreases by approximately 1 wavenumber.

Metal-Free Porphyrin−HRP. The fact that the amide I/I′ band position is not changed by the substitution of the heme for metal-free porphyrin shows that the secondary structure of the protein structure is not changed drastically. However, the increased contribution of the 1646 cm^{-1} component band in the resolution-enhanced spectrum of MP−HRP (Figure 2a.) indicates a slight loosening of the protein structure in the substituted form. This partial destabilization can be attributed to the soft regions of the protein, which reorganize or increase due to the heme substitution.

The structural difference between the native and the MP−HRP, reflected by the A_{1659}/A_{1647} ratio, disappears with increasing pressure. This fact indicates again that the substitution affects only the most soft region of the protein, which is destabilized by pressure below 5 kbar. Above 5 kbar the pressure-induced structural effects are determined by the hard part of the protein, which shows a very similar behavior in both the native and the MP−HRP. The soft regions are therefore slightly affected by the heme substitution, which can explain the decreased binding constant of aromatic substrates to the MP−HRP (*56*). Since the heme substitution does not change the structure of the protein significantly, the results of luminescence experiments performed on substituted proteins in the low-pressure range can provide relevant information, which can be extrapolated to the native enzyme.

Apo HRP. The removal of the heme seriously decreases the amount of ordered secondary structure in HRP. However, the existence of a sigmoid transition in the maximum position of the amide I/I′ band shows that there are ordered domains present in the protein, which conserve their spatial structure in the apoenzyme up to considerably high pressure. The unfolding effect of this folded core can be identified around 10.4 kbar. Considering only the unfolding pressure, the apoHRP is almost as pressure stable as the native form and the metal-free porphyrin form of the protein.

These observations can be explained by assuming that there is a rigid skeleton or a rigid core of the protein, which remains intact after the removal of the heme. A soft part will, however, loose its helical content upon removal of the heme. That is why the structure of apoHRP contains a smaller amount of folded structures. The fact that heme removal destabilizes the soft part indicates that the soft part is located around the heme pocket. The soft domain around the active site in the native protein allows structural fluctuations with high amplitude, probably opening and closing the heme pocket, allowing the substrate molecules to reach and leave the heme pocket. This hypothesis is in accordance with recent high-pressure experiments, which pointed out the existence of domains of different compressibilty in HRP (*32*). On the basis of infrared measurements, it is not possible to decide which part of the protein is the soft and which is the hard one. Recent molecular dynamic calculations on HRP in our laboratory (manuscript submitted), however, show that the molecular movements in the region with loop structures have higher amplitude, which can be attributed to the soft domain.

It can also explain the reduced cooperativity of the pressure unfolding, reflected in the broader transition region compared to the native protein.

The high stability of the rigid domain can be associated with four disulfide bonds, which increase the activation volume of the unfolding, due to restricting the movements of the folded helices as a whole. The high-pressure stability of the apoprotein is in contrast with myoglobin, where the apo form has considerably lower unfolding pressure than the native form (1.5 compared to 6 kbar (*57*)). This observation, together with the comparison of the pressure stability of the MP−HRP and the native HRP, suggests that HRP is a better object for the fluorescence studies than myoglobin because the heme substitution does not change the interactions, which are crucial for the overall stability of the protein structure.

Ca^{2+} Removal. It is known that Ca^{2+} is required to maintain the biochemically active environment of the heme. Presence of Ca^{2+} ions is also needed for the proper folding of the denatured HRP molecule (*58*, *59*).

One can notice that the maximum positions of the amide I/I′ bands are slightly lower in the absence of Ca^{2+}. A small reorganization can also be concluded from the lower A_{1659}/A_{1647} values of the Ca^{2+}-free protein (Table 1). The shift of the maximum position into the direction which is characteristic for the disordered structure indicates that the secondary structure contains less helices if Ca^{2+} is removed by EDTA. The initial rapid shift in case of the Ca^{2+}-free enzyme is caused by the hydrogen−deuterium exchange because it is accompanied by the decrease in the amide II band intensity. This again shows increased flexibility of the protein due to Ca^{2+} removal.

A more pronounced effect was observed on the pressure stability of HRP by EDTA treatment. The observed lowering of the denaturation pressure (by 2 kbar) can be explained in such a way: that the absence of the Ca^{2+} weakens the protein structure, allowing increased penetration of the water into the protein interior. The removal of Ca^{2+} is now shown to influence the secondary and tertiary structure of the enzyme in such a way, that it reduces the pressure stability.

Pressure induced the increase in the intensity of the 1588 cm^{-1} band at 2 kbar. This band is assigned to the Ca^{2+} free antisymmetric stretching mode of the carboxylate groups of the protein (*25*). The increase of this band at 2 kbar indicates that the Ca^{2+} removal at ambient pressure was probably not complete. Pressure is known to squeeze the water into the protein (*60*). At 2 kbar this elastic effect reaches probably the point, where the second Ca^{2+} is also accessible for the chelator molecule. An alternative explanation would be that Ca^{2+} is released due to elastic distortions of the tertiary structure. If this were the case, the pressure stability of the EDTA treated HRP would not have been lower than that of the native one.

Effect of BHA Binding to HRP. According to the slightly increased A_{1659}/A_{1647} intensity ratio upon ligand binding, the BHA-bound protein shows a more ordered structure compared to the native one. This agrees with the found X-ray structure (*16*), where two of the 12 α-helices are elongated in case of the BHA binding. The increase found in our infrared study is, however, higher (3% corresponding to

about 10 amino acids) than the one found by X-ray (1% corresponding to 2 amino acids).

HRP becomes denatured at a slightly reduced pressure when BHA is bound. The unfolding pressure is between that of the native and the Ca^{2+}-free forms.

The effect of BHA binding on the stability is peculiar. It is a common feature that the stability of a protein is increased upon substrate binding. At atmospheric pressure, the structure of HRP becomes more ordered, as seen from the increased contribution of the 1659 cm^{-1} band. Despite the increased helical content shown by the BHA-bound protein, the maximum position of the amide I/I′ band decreases more rapidly with pressure compared to the native and the substituted enzymes. Also, the unfolding pressure of the substrate-bound protein is lower compared to the native one. In these respects the stability is decreased. The paradox can be solved by assuming that the softer domain is around the heme pocket, which is stabilized by the substrate, but this soft domain is distorted below the total unfolding. This distortion includes squeezing water into the interior of this domain. The substrate binding is stabilized by hydrophobic interactions, and therefore, the presence of water can destabilize the structure. This might lead to the decrease in the unfolding pressure of the BHA-bound HRP. This explanation agrees with the finding of hole burning experiments where the compressibility of HRP-MP was increased by almost a factor of 3 when a substrate similar to BHA was bound to the porphyrin (*61*).

Effect of Reduction of the Disulfide Bonds. There are four disulfide bonds in the molecule (*14*): $Cys^{11}-Cys^{91}$, $Cys^{44}-Cys^{49}$, $Cys^{97}-Cys^{301}$, and $Cys^{177}-Cys^{209}$. By adding the reducing agent DTE the spectral changes are small. However the A_{1659}/A_{1647} ratio is reduced in the resolution enhanced spectrum, which indicates unfolding of a small part of the helical secondary structure. The decrease is much less than in the case of the apoprotein, but still higher than that of caused by the Ca^{2+} removal. It has to be noted, however, that as the reducing agent was added to the folded protein, it is not ensured that all of the disulfide bonds are already reduced at atmospheric pressure. Observing the crystal structure, one can see, that the $Cys^{44}-Cys^{49}$ and $Cys^{97}-Cys^{301}$ bonds are quite buried inside the protein, so they may not be accessible to DTE at ambient conditions, but only after partial loosening of the structure.

Disulfide bonds are present in some of the high-pressure stable proteins (*53*). If they were responsible for the pressure stability, one would expect that reducing them decreases the pressure stability dramatically. This is, however, not the case in our experiments. Cleavage of the disulfide bonds did change the unfolding pressure, from 12 to 9.5 kbar. Average proteins have an unfolding pressure of 5−6 kbar (*1*). In that respect the midpoint of unfolding at 9.5 kbar in the case of reduced HRP is still high, although it is the lowest among the HRP variants studied in this work. One of the explanations is that not all of the disulfide bonds are reduced in the native protein at atmospheric pressure, and local unfolding is needed to allow the DTE to reach the cysteins. This, however, would make the unfolding process more cooperative because small initial loosening of the structure could lead to further reduction and consequent unfolding. From the data shown in Figure 8 and comparison with the similar figures of the other HRP variants, we conclude that this is not the case. Denisov et al. (*62*) suggested that cleavage of the disulfide bonds leads to a state that has a higher flexibility rather than a changed structure. The increased flexibility is supported by the fact that there is practically no change in the amide II region upon pressurizing; i.e., the hydrogen−deuterium exchange is already completed at ambient pressure, even in the parts of the protein, which are inaccessible for the water at ambient conditions in the native enzyme. The observed aggregation of this form after the release of the pressure suggests that a more flexible intermediate is involved which could lead to increased intermolecular interactions.

Finally, one should also point out that HRP contains polysaccharide chains which may also play role in the stabilization of the molecule. It has been shown (*63*) that the recombinant form of HRP which did not contain the polysaccharide part of the molecule was less stable than the wild-type protein, already at conditions close to ambient ones. Because none of the effects studied by us (heme substitution, Ca^{2+} removal, substrate binding, reduction of the disulfide bonds) reduced the pressure stability to a value comparable with unfolding pressure of an average protein, we can conclude, that the carbohydrate shell may also contribute to the stability of the molecule. On the other hand, Dumoulin et al. found only a 15% decrease of the pressure stability of unglycosylated carboxypeptidase Y compared to the wild type (*64*). Further studies are needed to resolve a possible contribution of the bound carbohydrates to the stability.

CONCLUSIONS

The studied modifications of the HRP do not induce marked spectral changes in the FTIR spectra of the protein. This made it worthwhile to measure the pressure stability of the proteins. We used high pressure as a tool to perturb the modified proteins, to disclose the small structural alterations which cannot be seen directly at atmospheric pressure.

The pressure behavior of HRP was different in the range up to 5 kbar and between 6 and 10 kbar. Partial loosening of the soft domains of the molecule is observed below 5 kbar, but the rigid core of the molecule stabilizes the rest of the secondary structure up to quite high pressures. The pressure range, where different destabilized forms of HRP unfold (from 9.5 for the cleaved one, to 12 kbar for the native one), is quite high compared to other proteins. The four disulfide bonds stabilizing the tertiary structure of HRP can only be partially responsible for the relatively high-pressure stability of this protein, but our studies show that removal of Ca^{2+} or of the heme also have a destabilizing effect. The native HRP was found to have the highest stability. The heme substitution did not decrease the unfolding pressure significantly, but analysis of the spectra shows a decrease in the helical secondary structure content. Ca^{2+} removal by EDTA and BHA binding both decreased the stability. While the Ca^{2+} removal caused a larger shift in the denaturation pressure, the BHA binding affected the secondary structure much more.

None of the destabilizing effects led to drastic drop of the pressure stability, which implies, that a more complex mechanism is responsible for this high stability. It needs to be experimentally confirmed whether the carbohydrate moiety also contributes to the stability of the protein.

REFERENCES

1. Heremans, K., and Smeller, L. (1998) *Biochim. Biophys. Acta 1386*, 353−370.
2. Taniguchi, Y., Stanley, H. E., and Ludwig, H., Eds. (2002) in *Biological Systems under Extreme Conditions*, Springer-Verlag, Heidelberg.
3. Frauenfelder, H., Alberding, N. A., Ansari, A., Braunstein, D., Cowen, B. R., Hong, M. K., Iben, I. E. T., Johnson, J. B., Luck, S., Marden, M. C., Mourant, J. R., Ormos, P., Reinisch, L., Scholl, R., Schulte, A., Shyamsunder, E., Sorensen, L. B., Steinbach, P. J., Xie, A., Young, R. D., and Yue, K. T., (1990) *J. Phys. Chem. 94*, 1024−1037.
4. Köhler, M., Friedrich, J., and Fidy J. (1998) *Biochim. Biophys. Acta 1386*, 255−288.
5. Smeller, L., Rubens, P., and Heremans, K. (1999) *Biochemistry 38*, 3816−3820.
6. Zhang, J., Peng, X. A., and Jonas, J. (1995) *Biochemsitry 34*, 8631−8641.
7. Kunugi, S., Kitayaki, M., Yanagi, Y., Tanaka, N., Lange, R., and Balny C. (1997) *Eur. J. Biochem. 248*, 567−674.
8. Takeda, N., Kato, M., and Taniguchi Y. (1995) *Biochemistry 34*, 5980−5987.
9. Balny, C., and Masson, P. (1993) *Food Rev Int. 9*, 611−628
10. Smeller, L. (2002) *Biochim. Biophys. Acta 1595*, 11−29.
11. Morild, E. (1981) *Adv. Prot. Chem. 34*, 93−166.
12. Cooper, A. (1973) *Proc. Natl. Acad. Sci. U.S.A. 73*, 2740−2741.
13. Zollfrank, J., Friedrich, J., Fidy J., and Vanderkooi, J. M. (1991) *J. Chem. Phys. 94*, 8600−8603.
14. Gajhede, M., Schuller, D. J., Henriksen, A., Smith, A. T., and Poulos, T. L. (1997) *Nat. Struct. Biol. 4*, 1032−1038.
15. Schay, G., Galántai, R., Laberge, M., and Fidy, J. (2001) *Int. J. Quantum Chem. 84*, 290−301.
16. Henriksen, A., Schuller, D. J., Meno, K., Welinder, K. G., Smith, A. T., Gajhede, M. (1998) *Biochemistry 37*, 8054−8060.
17. Henriksen, A., Smith, A. T., and Gajhede, M. (1999) *J. Biol. Chem. 274*, 35005−35011.
18. Morishima, I., Kurono, M., and Shiro, Y. (1986) *J. Biol. Chem. 261*, 9391−9399.
19. Haschke, R. H. Freidhoff, J. M. (1978) *Biochem. Biophys. Res. Comm. 80*, 1039−1042.
20. Ogawa, S., Shiro, Y., and Morishima, I., (1979) *Biochem. Biophys. Res. Commun. 90*, 674−678.
21. Holzbaur, I. E., English, A. M., and Ismail A. A. (1996) *Biochemistry 35*, 5488−5494.
22. Ogunmola, B. B., Zipp, A., Chen, F., and Kauzmann, W. (1977) *Proc. Natl. Acad. Sci. U.S.A. 74*, 1−4.
23. Chattopadhyay, K., and Mazumdar, S. (2000) *Biochemistry 39*, 263−270.
24. Pina, D. G., Shnyrova, A. V., Gavilanes, F., Rodrigez, A., Leal, F., Roig, M. G., Shakharov, I. Y., Zadan, G. G, Villar, E., and Shnyrov, V. L. (2001) *Eur. J. Biochem. 268*, 120−126.
25. Kaposi, A. D., Fidy, J., Manas, E. S., Vanderkooi, J. M., and Wright, W. W. (1999) *Biochim. Biophys. Acta 1435*, 41−50.
26. Hendrickx, M., Ludikhuyze, L., Van den Broeck, I., and Weemaes, C. (1998) *Trends Food Sci. Technol. 9*, 197−203.
27. Rastogi, N. K., Eshtiaghi, M. N., and Knorr, D. (1999) *Food Biotechnol. 13*, 195−208.
28. Indrawati, VanLoey, A., Denys, S., and Hendrickx, M. (1998) *Food Biotechnol. 12*, 263−277.
29. Kaposi, A. D., Fidy, J., Stavrov, S. S., and Vanderkooi J. M. (1993) *J. Phys. Chem. 97*, 6319−6327.
30. Zollfrank, J., Friedrich, J., Fidy, J., and Vanderkooi, J. M. (1991) *J. Chem. Phys. 94*, 8600−8603.
31. Zollfrank, J., Friedrich, J., and Parak F. (1992) *Biophys. J. 61*, 716−724.
32. Smeller, L., and Fidy, J. (2002) *Biophys J. 82*, 426−436
33. Paul, K. G. (1958) *Acta Chem. Stand. 12*, 1312−1318.
34. Teale, F. W. J. (1959) *Biochim. Biophys. Acta 35*, 543−544.
35. Wong, P. T. T., and Moffat, D. J. (1989) *Appl. Spectrosc. 43*, 1279−1281.
36. Kauppinen, J. K., Moffat, D. J., Mantsch, H. H., and Cameron D. G. (1981) *Appl. Spectrosc. 35*, 271−276.
37. Smeller, L., Goossens, K and Heremans, K. (1995) *Appl. Spectrosc. 49*, 1538−1542.
38. Bandekar J. (1992) *Biochim. Biophys. Acta 1120*, 123−143.
39. Rahmelow, K., Huber, W., and Ackermann Th. (1998) *Anal. Biochem. 257*, 1−11.
40. Susi, H., and Byler D. M. (1986) *Methodol. Enzymol. 130*, 290−311.
41. Smeller, L. Goossens, K., and K. Heremans. (1995) *Vibr. Spectrosc. 8*, 199−203.
42. Dong, A. C., Randolph, T. W., and Carpenter J. F. (2000) *J. Biol. Chem. 275*, 27689−27693.
43. Heremans, K., Goossens, K., and Smeller, L. (1996) in *High-Pressure Effects in Molecular Biophysics* (Markley, J.L., Northrop, D. B., Royer, C. A., Eds.) pp 44−61, Oxford University Press, New York.
44. Panick G and Winter R. (2000) *Biochemistry 39*, 1862−1869.
45. Byler, D. M., and Susi H. (1986) *Biopolymers 25*, 469−487.
46. Dousseau, F., and Pezolet, M. (1990) *Biochemistry 29*, 8771−8779.
47. Harris, P. I., and Chapman, D. (1995) *Biopolymers 37*, 251−263.
48. Krimm, S., and Bandekar, J. (1980). *Biopolymers 19*, 1−29.
49. Heinisch, O., Kowalski, E., Goossens, K., Frank, J., Heremans, K., Ludwig, H., and Tauscher, B. (1995) *Z. Lebensm. Unters. Forsch. 201*, 562−565.
50. Lesch, H., Stadlbauer, H., Friedrich, J., Vanderkooi, J. M. (2002) *Biophys. J. 82*, 1644−1653.
51. St John, R. J., Carpenter, J. F., Balny, C., Randolph, T. W. (2001) *J. Biol. Chem. 276*, 46856−46863.
52. Panick, G., Malessa, R., Winter, R., Rapp, G., Frye. K. J., and Royer, C. A. (1998) *J. Mol Biol. 275*, 389−402.
53. Goossens K., Smeller L., Frank J., and Heremans K. (1996) *Eur. J. Biochem. 236*, 254−262.
54. Fusi, P., Goossens, K., Consonni, R., Grisa, M., Puricelli, P., Vecchio, G., Vanoni, M., Zetta, L., Heremans, K., and Tortora, P. (1997) *Proteins Struct. Funct. Genet. 29*, 381−390.
55. Zakin, M. R., and Hersbach, D. R. (1986) *J. Chem Phys 85*, 2376−2383.
56. Horie, T., Vanderkooi, J. M., and Paul, K.-G. (1985) *Biochemistry 24*, 7931.
57. Smeller L., Goossens K., and Heremans K. (1996) in *High-Pressure Science and Technology* (Trzeciakowski, W. A., Ed.) pp 863−865, World Scientific Co., Singapore.
58. Smith A. T. (1990) *J. Biol. Chem. 265*, 13335−13343.
59. Shiro, Y. Kurono, M. Morishima, I. (1986) *J. Biol. Chem. 261*, 9382−9390.
60. Wroblowski B, Diaz JF, Heremans K, Engelborghs Y. (1996) *Proteins Struct. Funct. Genet.* 25: 446−455.
61. Fidy, J., Vanderkooi, J. M., Zollfrank, J., and Friedrich, J. (1992) *Biophys. J. 63*, 1605−1612.
62. Denisov, V. P., Jonsson, B.-H., and Halle, B. (1999) *Nat. Struct. Biol.*, 6 253−260.
63. Gazaryan, I. G., Klyachko, N. L., Dulkis, Y. K., Ouporov I. V., and Levashov A. V. (1997) *Biochem. J. 328*, 643−647.
64. Dumoulin, M., Ueno, H., Hayashi, R., and Balny, C. (1999) *Eur. J. Biochem. 262*, 475−483.

BI026192N